Calibration for a Coaxial-loaded Cut-off Circular Waveguide with SOL Termination, and Related Application to Dielectric Measurement for Liquids*

Kouji SHIBATA†

ABSTRACT

In this study, termination with conditions referred to as short, open and loaded (SOL) as generally applied to S_{11} calibration for vector network analyzers (VNAs) was used for S_{11} calibration at the front of samples with a coaxial-feed-type cut-off circular waveguide (jig) as a preliminary step for dielectric measurement in liquids. The equations for single jig port calibration of S_{11} with three termination conditions were first defined, and a new S_{11} calibration theory with SOL conditions especially for the cut-off circular waveguide was proposed along with a method for termination with a coaxial-feed-type matched load inside the cut-off circular waveguide. The reflection characteristics and reproducibility of the proposed termination in repeated measurements were observed over the frequency band of 0.50 – 3.0 GHz. S_{11} for the front surface of the sample material was measured with each SOL condition and various liquids in the jig after SOL calibration using a coaxial-feed-type cut-off circular waveguide at frequencies of 0.50, 1.5 and 3.0 GHz. S_{11} values calibrated with SOL conditions were then compared with those from SOM (short, open and one reference material) conditions, with results indicating close agreement suggesting the validity of the proposed method. The dielectric constants of various liquids were also estimated as an inverse problem based on comparison of S_{11} calculated from an analytical model using EM analysis via the MM (mode-matching) technique with measured S_{11} values after SOL calibration as described above. The effectiveness of the method was verified via comparison with dielectric constants estimated after S_{11} calibration with SOM termination. The frequency characteristics of complex permittivity for various liquids estimated as an inverse problem based on the MM technique at 0.50 to 3.0 GHz after S_{11} calibration with SOL were additionally compared with those estimated after SOM calibration, with results showing favorable agreement. The study's outcomes indicated the validity of the proposed S_{11} calibration and dielectric constant estimation approaches.

Key Words: *Dielectric measurement, Liquid, Impedance measurement, Coaxial line, Cut-off circular waveguide reflection method, Microwave, Radio frequency, S11, calibration*

1. Introduction

Shibata (2010) previously outlined the effectiveness of high-precision broadband dielectric measurement for small amounts of certain liquids based on a reflection constant using a coaxial-feed-type open-ended cut-off circular waveguide [1]. As part of efforts to develop this method, the potential for dielectric measurement in liquids in the low frequency band, estimation using a simple formula, calculation for

* 令和 5 年 12 月 1 日 受付

† 工学研究科工学専攻・教授

uncertainty and methods for improving measurement accuracy have also been presented [2] – [7]. However, these approaches produce an error effect on S_{11} and the dielectric constant caused by the difference between the actual dimensions of the jig and the analytical model. Against this background, a method enabling S_{11} calibration for a cut-off circular waveguide loaded coaxial line using a vector network analyzer (VNA) with pure water, methanol and air as reference materials and no short termination was also proposed by Shibata (2019), with effectiveness verified from electromagnetic (EM) analysis and comparison with S_{11} values obtained using another S_{11} calibration method [8]. The dielectric constant estimated as an inverse problem based on comparison of S_{11} calculation from EM analysis [1] with various liquids inserted and from the above S_{11} values after calibration with three reference materials was then compared with dielectric constants determined using conventional methods [9]. The results indicated close agreement, thereby underlining the validity of the proposed technique [8], [9]. A method for calibration of S_{11} at the front of the sample using SOM conditions with a cut-off circular waveguide (jig) after mounting in the measurement system and before dielectric measurement has also been proposed [10], with effectiveness verified via comparison with results from another method. The dielectric constant estimated with various liquids inserted and from the above S_{11} values after SOM calibration were compared with dielectric constants determined using conventional methods [9], and the reversibility of the method was verified using methanol as the reference material. The results showed close agreement, indicating the validity of the proposed method [10], [11]. In this approach, a reference liquid is used instead of matched load termination as a calibrator for S_{11} calibration. However, it is known that the complex permittivity of liquids changes significantly with the incorporation of airborne moisture into the reference material (methanol or ethanol) and the effects of reduced liquid temperature caused by vaporization [7], [11]. Accordingly, S_{11} measurement accuracy may be impaired by input impedance differences caused by changes in liquid temperature.

In this study, SOL (short, open and loaded) termination conditions were used instead of reference liquids for calibration of S_{11} at the front of the sample with a coaxial-feed-type cut-off circular waveguide for insertion of the test material, with the dielectric constant estimated from the S_{11} value determined using a VNA. To this end, the equations for single jig port calibration of S_{11} with three termination conditions were first defined, and the calibration method with SOL conditions was presented. A structure to realize a coaxial-feed-type matched load termination in a cut-off circular waveguide was also proposed, with validity and reproducibility verified via repeated measurement over the frequency band of 0.50 – 3.0 GHz. S_{11} for the jig was also calibrated from the reflection constant with SOL terminations using a VNA over the same frequency band, and the value at the front surface of the sample was measured with each termination condition and various liquids in the jig. The validity of the values determined with the proposed method was verified via comparison with S_{11} measured after SOM calibration conditions [10]. The dielectric constants of various liquids were also estimated based on an inverse problem approach involving comparison with the S_{11} value calculated using EM analysis via the MM technique [1] from the above S_{11} value after calibration with SOL conditions at frequencies of 0.50, 1.5 and 3.0 GHz. The results were compared with the dielectric constant values estimated as an inverse problem based on the MM technique after SOM calibration [11], with results showing favorable agreement. After calibration of S_{11} with SOL conditions, the results of estimation to determine the dielectric constants of various liquids were compared with the results of dielectric constant estimation after calibration of S_{11} with SOM conditions and frequency characteristics of 0.50 to 3.0 GHz. The results indicated correspondence with a certain margin of error. The validity of the proposed S_{11} calibration approach and the dielectric constant estimation method was thus confirmed.

2. Dielectric measurement in liquids and related S_{11} calibration theory

In this approach, the dielectric constant of a material is estimated by comparing the measured S_{11} value against the result of calculation with various liquids in the jig (Fig. 1). Here, S_{11} calibration with the use of SOL termination conditions [12] – [14] is usually adopted in one-port calibration for a coaxial interface in the preliminary step for dielectric measurement in liquids. The estimation procedure is as follows:

1. The measurement jig (a coaxial-feed-type cut-off circular waveguide with an SMA connector) is attached to a measurement cable connected to a VNA.

2. S_{11} is calibrated at the front surface of the jig sample with SOL termination conditions.

3. S_{11} at the front of the sample material is measured with various liquids in the jig.

4. The dielectric constant is estimated as an inverse problem so that the calculated S_{11} value for the jig-related analytical model corresponds to the measured value for each frequency.

Here, S_{11} calibration is performed at the front of the inserted sample when the coaxial-feed type cut-off circular waveguide is used as a jig for dielectric measurement in liquids. A matched load is also used as a calibrator. Here, correction is needed in relation to the jig structure used for S_{11} calibration with this method. Specifically, a theoretical value for a reflection constant corresponding to the physical structure for each impedance standard is required for S_{11} calibration of the jig. In this study, the reflection constant for an open condition was calculated from an equivalent circuit [10] as determined by substituting the electrostatic capacitance observed at the tip of the coaxial line, as derived from comparison of reflection constants calculated from an analytical model using EM analysis as previously proposed [10]. The theoretical value for short termination was set as $\Gamma = -1$. Actual calibration for a short condition was then performed with the structure and procedure previously proposed [11]. The theoretical value for load termination was set as $\Gamma = 0$.

The procedure for manufacture of the coaxial-feed type matched load termination in the cut-off circular waveguide and the procedure for S_{11} calibration with load termination are outlined in the next chapter. In actual calibration work, S_{11} is first measured using a VNA with SOL termination conditions in the jig. S_{11} is then calibrated at the front surface of the sample by substituting the above theoretical reflection constant and the measured value of S_{11}. Here, the equations required for calibration of S_{11} with SOL termination conditions are defined as outlined below.

The reflection constant in Ref. 2 for the analysis model of Figs. 1 and 2 is calibrated [8], [10] from the measured reflection constant ρ_{meas} for Ref. 1 using Eq. (1).

$$\dot{\Gamma}_{corr} = \frac{\dot{\rho}_{meas} - \dot{E}_{DF}}{\dot{E}_{SF} \cdot \dot{\rho}_{meas} + \dot{E}_{RF} - \dot{E}_{SF} \cdot \dot{E}_{DF}} \quad (1)$$

Here, E_{SF}, E_{DF} and E_{RF} are system error terms required for S_{11} calibration as defined by Eqs. (2) to (4).

$$\dot{E}_{SF} = \frac{\dot{\rho}_2 - \dot{\rho}_3 + \dot{\gamma} \cdot \left(\dot{\Gamma}_3 - \dot{\Gamma}_2 \right)}{\dot{\Gamma}_2 \cdot \dot{\rho}_2 - \dot{\Gamma}_3 \cdot \dot{\rho}_3} \quad (2)$$

$$\dot{E}_{DF} = \dot{\rho}_1 - \dot{\Gamma}_1 \cdot \left(\dot{E}_{SF} \cdot \dot{\rho}_1 + \dot{\gamma} \right) \quad (3)$$

$$\dot{E}_{RF} = \dot{E}_{DF} \cdot \dot{E}_{SF} + \dot{\gamma} \quad (4)$$

The auxiliary function γ of the above values is defined by Eq. (5).

$$\dot{\gamma} = \frac{\left(\dot{\rho}_2 - \dot{\rho}_1 \right) \cdot \left(\dot{\Gamma}_2 \cdot \dot{\rho}_2 - \dot{\Gamma}_3 \cdot \dot{\rho}_3 \right) + \left(\dot{\rho}_2 - \dot{\rho}_3 \right) \cdot \left(\dot{\Gamma}_1 \cdot \dot{\rho}_1 - \dot{\Gamma}_2 \cdot \dot{\rho}_2 \right)}{\left(\dot{\Gamma}_3 - \dot{\Gamma}_2 \right) \cdot \left(\dot{\Gamma}_2 \cdot \dot{\rho}_2 - \dot{\Gamma}_1 \cdot \dot{\rho}_1 \right) + \left(\dot{\Gamma}_1 - \dot{\Gamma}_2 \right) \cdot \left(\dot{\Gamma}_3 \cdot \dot{\rho}_3 - \dot{\Gamma}_2 \cdot \dot{\rho}_2 \right)} \quad (5)$$

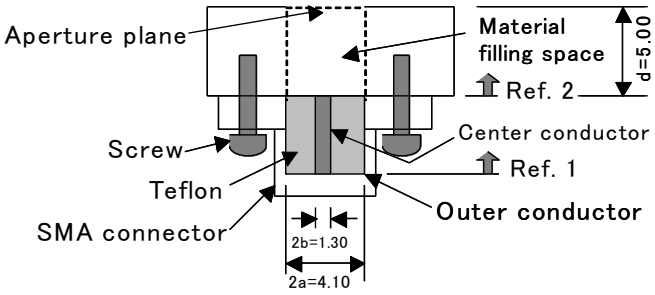

Figure 1. Jig cross section

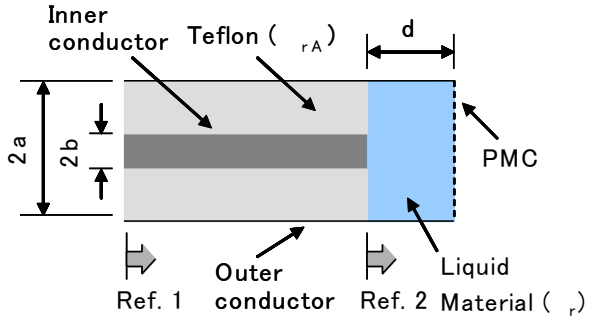

Figure 2. Analytical model

The open-ended coaxial line shown in Figs. 1 and 2 is represented by the equivalent circuit shown in Fig. 3, where C_f and $\varepsilon_{ri} \cdot C_0$ are the fringing capacitance at the tip of the coaxial line and the sample insertion section at the coaxial tip, respectively. Here, $C_T = C_f + \varepsilon_{ri} \cdot C_0$ is satisfied. The input impedance $Z_{\Gamma i}$ for Ref. 2 is expressed by

$$\dot{Z}_{\Gamma i} = \frac{1}{j\omega \cdot C_T} = \frac{1}{j\omega \cdot \left(C_f + \dot{\varepsilon}_{ri} \cdot C_o\right)} \quad (6)$$

The following equation for calculation of the reflection constant for Ref. 2 is then iterated [8], [10]:

$$\dot{\Gamma}_i = \frac{\dot{Z}_{\Gamma i} - Z_0}{\dot{Z}_{\Gamma i} + Z_0} = \frac{1 - j\omega C_0 \cdot \dot{\varepsilon}_{ri} \cdot Z_0 - j\omega C_f \cdot Z_0}{1 + j\omega C_0 \cdot \dot{\varepsilon}_{ri} \cdot Z_0 + j\omega C_f \cdot Z_0} \quad (7)$$

Here, Z_0 is the characteristic impedance of the coaxial line, defined as $Z_0 = 50\ \Omega$. Accordingly, the theoretical reflection coefficient Γ_i for Ref. 2 with the assumption of material insertion is also determined based on Eq. (7) by substituting C_f and C_0 for the equivalent circuit shown in Fig. 3. In the proposed method, to improve accuracy in measurement of S_{11} against the conventional method [12] – [14], C_f and C_0 in Eq. (6) are determined by substituting the input impedance calculated via the MM technique [1] for the analysis model of Fig. 2 at each frequency into $Z_{\Gamma i}$ on the left side [8]. Here, $Z_{\Gamma i}$ for open termination is determined by substituting $\varepsilon_{ri} = 1.0$ (air, where i = 2) into ε_{ri} in Eq. (6). The reflection constant for the open condition Γ_2 is thus determined by substituting $\varepsilon_{r2} = 1.0$ into ε_{ri} in Eq. (7). The reflection constants for short and load terminations are determined by substituting $\Gamma_1 = -1$ (where i = 1) and $\Gamma_3 = 0$ (where i = 3) into Γ_i on the right side of Eq. (7). Accordingly, E_{DF}, E_{RF} and E_{SF} (system errors in Eq. (1)) are determined based on Eqs. (2) – (5) from the theoretical reflection constant Γ_i (where i = 1, 2 and 3) of the reflection coefficient under the three termination conditions in Ref. 2 and the measured reflection coefficient ρ_i for Ref. 1. From the above relationship, the calibrated reflection coefficient Γ_{corr} for Ref. 2 is determined by substituting the measured ρ_{meas} value for Ref. 1 and the E_{DF}, E_{RF} and E_{SF} values determined from the three termination conditions into Eq. (1). References [8] and [10] detail the procedure for determination of actual electrostatic capacitance C_0 and C_f in Eqs. (6) and (7) for calculation of the theoretical reflection constant based on the equivalent circuit and the theory of S_{11} calibration.

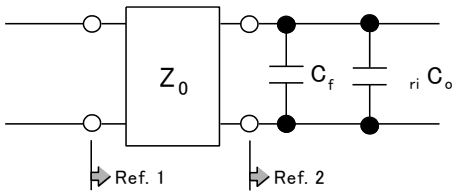

Figure 3. Analytical model equivalent circuit

3. Matched load in a cut-off circular waveguide

This chapter outlines realization for matched loading in the cut-off circular waveguide for one-port S_{11} calibration using SOL conditions via the procedure described in Chapter 2. For this purpose, the dimensions and electrical constants of the jig as shown in Figs. 1 and 2 were set as 2a = 4.10 mm, 2b = 1.30 mm, d = 5.00 mm and $\varepsilon_{rA} = 2.05$. Here, accurate connection of the matched load termination on the flange surface of the coaxial line is challenging when the coaxial probe [15], [16] is used in dielectric measurement for a high-loss electrical material. Accordingly, a reference material is generally used instead of the matched load for S_{11} calibration of the coaxial probe [15], [16]. Meanwhile, a coaxial-connector-feed-type matched load is posed as the dummy load. This approach is generally used for S_{11} calibration. In this study, a matched load was fabricated inside the coaxial-loaded-type cut-off circular waveguide. For this purpose, the same SMA connector type (BL52-1201-01, Orient Microwave Corp.) as that applied with the jig for dielectric measurement (Fig. 1) was used. The center conductor at the tip of the connector and the PTFE resin for electrical isolation from the center conductor were cut to the depth of the jig (d = 5.0 mm), and an SMA-type dummy load was attached to the coaxial connector (Fig. 4). In actual load calibration, a metal spacer (known as a shim) was attached to the flange surface of the connector to improve electrical contact. The tip of the connector was put into the insertion hole of the jig for dielectric measurement (Fig. 5).

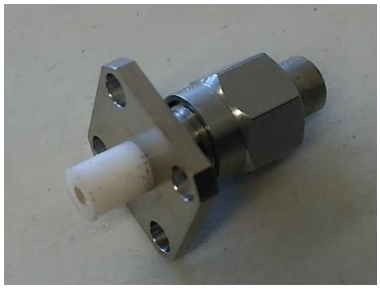

Figure 4. SMA connector with dummy load

Figure 5. SMA connector insertion into the jig

The jig (Fig. 6) was attached to the tip of the coaxial cable, and the newly created auxiliary jig was placed as shown in Fig. 7. Pressure was applied to the SMA connector by tightening the screw, and S_{11} calibration

was performed using the assembly combining the jig for dielectric measurement and the matched load as described above.

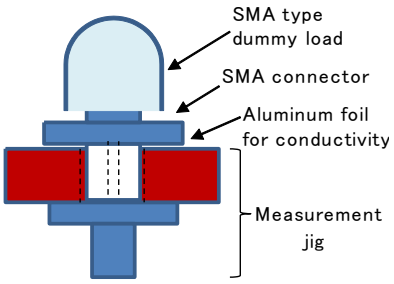

Figure 6. Cross-section of the dielectric measurement jig with matched load attached

Figure 7. Dielectric measurement jig attached to the pressure-application jig

The reflection constant characteristic of the matched load fabricated via the above procedure was verified over the frequency band of 0.5 – 3.0 GHz. To this end, the pre-jig-mounting tip of the measurement cable connected to the VNA was first calibrated using a general SMA connector-type SOL calibration kit, and the matched load and pressure-application jig were attached to the cable. The S_{11} frequency characteristics of the jigs were evaluated as scalar quantities. Specifically, the relationship between the input impedance (where $Z_0 = 50\ \Omega$) and the reflection constant are expressed by Eq. (7). The return loss [dB] of the jigs was calculated as $20\log(|\Gamma_i|)$ from the measured reflection constant Γ_i. S_{11} measurement was conducted four times (Fig. 8), and the return loss was less than –30 dB over the frequency band of 0.50 – 3.0 GHz. The results indicated improved electrical contact between the outer-conductor grounds of the coaxial line due to insertion of the metal shim and the realization of favorable matched loading based on the proposed procedure.

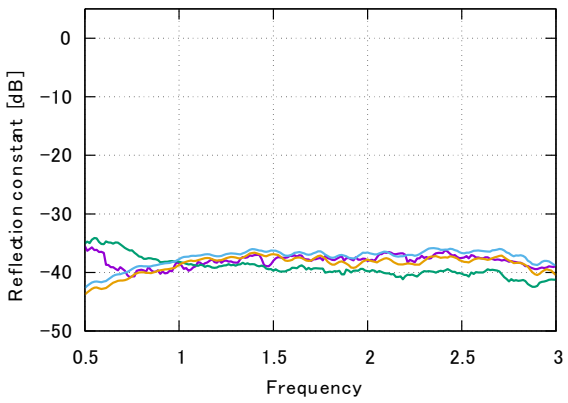

Figure 8. Return loss [dB] variations in matched loading

4. Verification of the S_{11} calibration theory and the proposed matched loading

This chapter discusses the validity of S_{11} calibration for a coaxial-loaded cut-off circular waveguide using SOL conditions and the newly created matched load described in Chapters 2 and 3. Verification was performed at frequencies of 0.50, 1.5 and 3.0 GHz with dimensions and electrical constants for the sample insertion hole set as 2a = 4.10 mm, 2b = 1.30 mm, d = 5.0 mm and $\varepsilon_{rm} = 2.05$ in the analytical model (Figs. 1 and 2). The jig shown in Fig. 1 was attached to the tip of the coaxial cable after calibration with a general SMA connector-type SOL calibration kit, and the reflection constant of Ref. 1 (Figs. 1 to 3) with SOL termination conditions was measured. The resulting values were substituted for ρ_i (where i = 1, 2 and 3) in Eqs. (2) – (5), and the theoretical reflection coefficient Γ_i (Ref. 2) with SOL conditions as calculated using Eq. (7) was also substituted into Γ_i. Input impedance measured on the SOL calibration plane (Ref. 1) converted to a reflection coefficient with short, open and matched loading as unknown terminations and various liquids inserted as unknown materials was also substituted for ρ_{meas} in Eq. (1). Pure water, methanol and ethanol were the unknown materials. The reflection coefficient at the front of the sample after calibration (Ref. 2) under each termination condition was thus calculated as Γ_{corr}.

The measured values of S_{11} for each termination condition at the frequencies of 0.50, 1.5 and 3.0 GHz were compared with those after calibration with SOM conditions as previously proposed [10]. The results of input impedance measurement for short, open and loaded termination conditions are shown in Table 1 (a). The differences after calibration were within 3.2% with short, 2.0% with methanol and 3.2% with air (open) conditions, indicating close agreement. Values measured with loading after calibration with each method also matched within a difference of 1.6% for the real part. The percentage for loading was relatively large in the imaginary part, but measured values for this part after calibration were close to the theoretical value (0.0). Measured values of input impedance with various liquids inserted are shown in Table 1 (b). Values with pure water after calibration with each method also matched within a difference of 1.9% for the imaginary part, while the percentage was relatively large at 42% for the real part. However, the actual impedance difference was 1.45. The difference in the real part is attributed to the measured input impedance with the third reference condition (loading for SOL and pure water for SOM) differing from the theoretical value. Measured values with methanol after calibration with each method also matched within a difference of 2.8% for the imaginary part, while the percentage was relatively large at 7.6% for the real part at a frequency of 0.50 GHz. The difference in the real part is attributed the same factors as for pure water. Measured values for methanol matched within a difference of 3.1% for both the real and imaginary parts over all frequency bands. This agreement is attributed to the high input impedance for the coaxial tip with ethanol inserted.

Table 1. Input impedance at the front of the sample (Ref. 2) for various termination conditions after each calibration

(a) SOL termination conditions

Condition		Frequency [GHz]		
		0.50	1.5	3.0
Short	Calibration with SOL	$+6.1288\cdot10^{-4}$ $+j\ 7.2523\cdot10^{-4}$	$+6.03099\cdot10^{-3}$ $+\ j\ 9.27912\cdot10^{-3}$	$+2.2188\cdot10^{-2}$ $-j\ 2.6631\cdot10^{-2}$
	Calibration with SOM [8]	$+5.3986\cdot10^{-4}$ $+j7.2591\cdot10^{-4}$	$5.88933\cdot10^{-3}$ $+\ j\ 9.47362\cdot10^{-3}$	$2.229770\cdot10^{-2}$ $-j\ 2.5828\cdot10^{-2}$
Inter-value difference [%]		+13.526 –0.094	+2.405 –2.053	–0.492 +3.109
Open	Calibration with SOL	–233.9972 –j 9611.9785	–9.241295 –j 3243.4902	–5.95029 –j 1603.468
	Calibration with SOM [8]	–232.47672 –j 9609.6846	–9.14556 –j 3243.3059	–5.73558 –j 1603.1008
Inter-value difference [%]		+0.654 +0.024	+1.047 +0.006	+3.743 +0.023
Load	Calibration with SOL	50.000011 $+j\ 7.13996\cdot10^{-6}$	49.999996 $+j\ 3.970464\cdot10^{-6}$	50.000000 $+j\ 1.0831\cdot10^{-6}$
	Calibration with SOM [8]	50.00866 +j 0.516533	50.400734 +j 1.020430	49.23812 +j 0.88838
Inter-value difference [%]		–0.017 –100.0	–0.795 –100.0	+1.547 –100.0

(b) With various liquids (25℃)

Condition		Frequency [GHz]		
		0.50	1.5	3.0
Pure water	Calibration with SOL	2.0148997 –j 142.7883	2.51052094 –j 46.4820	3.1531580 –j 22.3434
	Calibration with SOM [8]	3.468634 –j 142.7852	3.469366 –j 46.7847	3.485886 –j 21.9431
Inter-value difference [%]		–41.911 +0.002	–27.637 –0.647	–9.545 +1.824
Methanol	Calibration with SOL	38.118378 –j 311.9749	40.2270241 –j 106.14945	40.845867 –j 56.1719
	Calibration with SOM [8]	41.24409 –j 311.6437	42.63356 –j 106.1736	41.20242 –j 54.64313
Inter-value difference [%]		–7.579 +0.106	–5.645 –0.023	–0.865 +2.798
Ethanol	Calibration with SOL	151.27220 –j 415.066	145.187576 –j 173.5527	121.92667 –j 125.8806
	Calibration with SOM [8]	155.41959 –j 413.6861	149.69363 –j 172.2116	122.47092 –j 122.1180
Inter-value difference [%]		–2.669 +0.334	–3.010 +0.779	–0.444 +3.081

5. Dielectric measurement with various liquids

The dielectric constants of various liquids were estimated as an inverse problem based on comparison of S_{11} measured with an unknown material in the jig and that calculated using the MM technique with a similar analytical model [1] from input impedance measured with liquids in the jig after S_{11} calibration at the front of the sample using SOL conditions (as described in Chapter 4). The effectiveness of the proposed method was verified by comparing the above values with otherwise obtained outcomes after SOM calibration [11] and the theoretical value from the Debye relaxation equation [17] – [19]. The results of dielectric constant estimation for pure water are shown in Table 2 (a). Values estimated as an inverse problem via the MM technique after calibration with SOL were first compared with values estimated as an inverse problem via the MM technique after SOM calibration, with differences of no more than 1.3% for the real part at all frequencies. The percentage was relatively large at 42% for the imaginary part at a frequency of 0.50 GHz, but the actual permittivity difference was 0.80. Values estimated as an inverse problem via the MM technique after calibration with SOL conditions were compared with theoretical values obtained using the Debye dispersion formula, with results showing an exact match for all frequencies. This is attributed to the fact that the calibration procedure for S_{11} based on SOM involved the complex permittivity of pure water calculated using the Debye dispersion formula.

The results of dielectric constant estimation for methanol are shown in Table 2 (b). Values estimated as an inverse problem via the MM technique after SOL calibration were compared with those after SOM calibration, with results showing differences of no more than 1.4% for the real part and 7.6% for the imaginary part at all frequencies. Values estimated as an inverse problem via the MM technique after calibration with SOL and SOM conditions were also compared with theoretical values obtained using the Debye dispersion formula, with results showing large differences of up to 10.2% for the real part and up to 15% for the imaginary part. The estimated values for the real and imaginary parts as determined after calibration with SOL and SOM conditions were approximately 3.2 – 1.7 and 0.5 – 2.3 greater, respectively, than those obtained with the Debye relaxation formula. This is attributed to the incorporation of airborne moisture into methanol and a reduction of liquid temperature caused by methanol evaporation after insertion into the jig in actual measurement of S_{11}. The close agreement between estimation values after SOL and SOM calibration indicates the validity of the proposed S_{11} calibration with SOL and dielectric constant estimation.

The results of dielectric constant estimation for ethanol are shown in Table 2 (c). Values estimated as an inverse problem via the MM technique after SOL calibration were compared with those obtained after SOM calibration, showing differences of no more than 3.1% for both the real and imaginary parts at all frequencies. The estimated value for the real part as determined using the MM technique with ethanol was approximately 3.5 greater than that obtained with the Debye relaxation formula [19], and inter-value differences of more

than 6.9% for both the real and imaginary parts were observed at 0.50, 1.5 and 3.0 GHz. This is attributed to the incorporation of airborne moisture into ethanol and the effects of reduced liquid temperature caused by ethanol evaporation in actual measurement. The close agreement between estimation values after SOL and SOM calibration indicates the validity of the proposed S_{11} calibration with SOL and dielectric constant estimation.

Table 2. Results of complex permittivity estimation for various liquids

(a) Pure water

Condition	Frequency [GHz]		
	0.50	1.5	3.0
Inverse problem with MM technique after SOL calibration	78.5326 –j 1.1110	78.8041 –j 4.1913	75.8627 –j 9.8497
Inverse problem with MM technique after SOM calibration [11]	78.5036 –j 1.9119	78.1077 –j 5.7048	76.8026 –j 11.2056
Debye dispersion formula [17]	78.5036 –j 1.9119	78.1077 –j 5.7048	76.8026 –j 11.2056
Difference between estimation after SOL and SOM calibration [%]	+0.037 –41.890	+0.892 –26.530	–1.224 –12.100
Difference with MM technique after SOL calibration and Debye dispersion formula [%]	+0.037 –41.890	+0.892 –26.530	–1.224 –12.100
Difference between MM technique after SOM calibration and Debye dispersion formula [%]	0.0 0.0	0.0 0.0	0.0 0.0

(b) Methanol

Condition	Frequency [GHz]		
	0.50	1.5	3.0
Inverse problem with MM technique after SOL calibration	35.2660 –j 4.3479	30.4427 –j 11.5697	21.3290 –j 15.2521
Inverse problem with MM technique after SOM calibration [11]	35.2133 –j 4.7025	29.9752 –j 12.0730	21.3876 –j 15.8446
Debye dispersion formula [18], [19]	31.99033 –j 4.20683	27.62791 –j 10.5372	19.73333 –j 13.5342
Difference between estimation after SOL and SOM calibration [%]	+0.150 –7.541	+1.560 –4.169	–0.274 –3.739
Difference between MM technique after SOL calibration and Debye dispersion formula [%]	+10.240 +3.353	+10.188 +9.799	+8.086 +12.693
Difference between MM technique after SOM calibration and Debye dispersion formula [%]	+10.075 +11.783	+8.496 +14.575	+8.383 +17.071

(c) Ethanol

Condition	Frequency [GHz]		
	0.50	1.5	3.0
Inverse problem with MM technique after SOL calibration	23.6421 –j 8.7357	12.3906 –j 10.5899	7.3640 –j 7.3300
Inverse problem with MM technique after SOM calibration [11]	23.5467 –j 8.9693	12.0842 –j 10.7384	7.3366 –j 7.5607
Debye dispersion formula [19]	20.2060 –j 8.1717	10.3290 –j 9.1462	6.3698 –j 5.9713
Difference between estimation after SOL and SOM calibration [%]	+0.405 –2.604	+2.536 –1.383	+0.373 –3.051
Difference between MM technique after SOL calibration and Debye dispersion formula [%]	+17.005 +6.902	+19.959 +15.785	+15.608 +22.754
Difference between MM technique after SOM calibration and Debye dispersion formula [%]	+16.533 +9.761	+16.993 +17.408	+15.178 +26.617

6. Frequency characteristics of complex permittivity in various liquids

Differences in dielectric constants with the individual S_{11} calibration conditions described in the previous chapter were examined at frequencies of 0.50 to 3.0 GHz, with pure water, methanol and ethanol at a liquid temperature of 25.0℃ as unknown materials. The results estimated as an inverse problem with the MM technique with pure water in the jig after application of the two calibration methods are shown in Fig. 9. Here, purple indicates the real part estimated as an inverse problem after SOL calibration, light blue indicates the real part estimated as an inverse problem after SOM calibration, yellow indicates the real part calculated from the Debye relaxation formula, green indicates the imaginary part estimated as an inverse problem after SOL calibration, orange indicates the imaginary part estimated as an inverse problem after SOL calibration, and blue indicates the imaginary part calculated from the Debye relaxation formula. Values estimated as an inverse problem via the MM technique after calibration with SOL and SOM termination were compared with theoretical values obtained using the Debye dispersion formula, with results showing favorable agreement for the real part at all frequencies. This is attributed to the fact that S_{11} calibration with SOM was performed using pure water as a reference material. The difference of 0.80 for the imaginary part at 0.50 GHz is attributed to variations in measured S_{11} values.

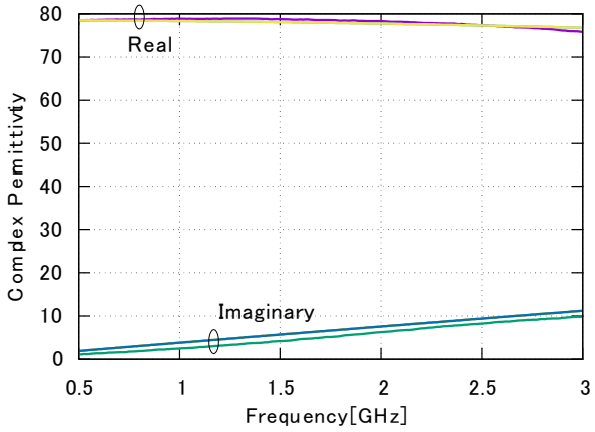

Figure 9. Frequency characteristics of complex permittivity for pure water

Frequency characteristics from the results of dielectric determination with methanol as an inverse problem using the MM technique after application of the two calibration methods are shown in Fig. 10, which also includes theoretical values calculated using the Debye relaxation method. Complex permittivity values estimated as an inverse problem after calibration with SOL and SOM matched within a difference of 1.4% for the real part and 7.6% for the imaginary part over all frequency bands. Values estimated for the real part and the imaginary part as determined after calibration with SOL and SOM were approximately 3.2 – 1.7 and 0.5 – 2.3 greater, respectively, than those obtained with the Debye relaxation formula. This is attributed to incorporation of airborne moisture into methanol and reduction of liquid temperature caused by methanol evaporation after insertion into the jig in actual S_{11} measurement. However, the close agreement between estimation values after SOL and SOM calibration indicates the validity of the proposed S_{11} calibration with SOL and dielectric constant estimation.

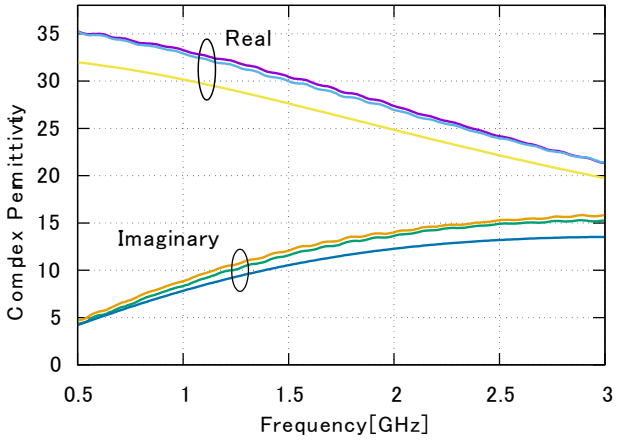

Figure 10. Frequency characteristics of complex permittivity for methanol

Frequency characteristics from the results of dielectric measurement with ethanol after application of the two calibration methods are shown in Fig. 11, which also shows theoretical values calculated using the Debye relaxation method. Complex permittivity values estimated as an inverse problem after calibration with SOL and SOM also matched within a difference of 1.6% for the real part and 7.6% for the imaginary part over all frequency bands. Values estimated for the real part and the imaginary part as determined after calibration with SOL and SOM were approximately 3.4 – 1.0 and 0.8 – 1.6 greater, respectively, than those obtained with the Debye relaxation formula. However, close agreement was observed between values estimated as an inverse problem after calibration with SOL and SOM conditions. These results indicated the validity of the proposed S_{11} calibration for a coaxial-loaded cut-off circular waveguide with SOL and dielectric constant estimation based on an inverse problem via the MM technique after calibration. Future work will involve comparison with the conventional coaxial probe method [19] − [21] and similar with variations relating to factors such as jig dimensions, VNA/measurement system specifications, S_{11} measurement theory and temperature changes. Clarification of measurement uncertainty [22] for the proposed method is also needed in comparison with the conventional method.

7. Conclusion

In this study, SOL (short, open and loaded) termination conditions were used instead of reference liquids for calibration of S_{11} at the front of the sample with a coaxial-feed-type cut-off circular waveguide for insertion of the test material, with the dielectric constant estimated from the S_{11} value determined using a VNA. To this end, the equations for single jig port calibration of S_{11} with three termination conditions were first defined, and the calibration method with SOL conditions was presented. A structure to realize a coaxial-feed-type matched load termination in a cut-off circular waveguide was also proposed, with validity and reproducibility verified via repeated measurement over the frequency band of 0.50 – 3.0 GHz. S_{11} for the jig was also calibrated from the reflection constant with SOL terminations using a VNA over the same frequency band, and the value at the front surface of the sample was measured with each termination condition and various liquids in the jig. The validity of the values determined with the proposed method was verified via comparison with S_{11} measured after SOM calibration conditions. The dielectric constants of various liquids were also estimated based on an inverse problem approach involving comparison with the S_{11} value calculated using EM analysis via the MM technique from the above S_{11} value after calibration with SOL conditions at frequencies of 0.50, 1.5 and 3.0 GHz. The results were compared with the dielectric constant values estimated as an inverse problem based on the MM technique after SOM calibration, with results showing favorable agreement. After calibration of S_{11} with SOL conditions, the results of estimation to determine the dielectric constants of various liquids were compared with the results of dielectric constant estimation after calibration of S_{11} with SOM conditions and frequency characteristics of 0.50 to 3.0 GHz.

The results indicated correspondence with a certain margin of error. The validity of the proposed S_{11} calibration approach and the dielectric constant estimation method was thus confirmed.

Future work will involve comparison with the conventional coaxial probe method [19] − [21] and similar with variations relating to factors such as jig dimensions, VNA/measurement system specifications, S_{11} measurement theory and temperature changes. Clarification of measurement uncertainty [22] for the proposed method is also needed in comparison with the conventional method.

Acknowledgements

This work was partly supported by a Japan Society for the Promotion of Science (JSPS) Kakenhi Grant (no. 20K04522) for the work titled Establishment of a Broadband Dielectric Measurement Method for Liquids in Temperature-Change Environments for Synthesis of Functional Materials.

References

[1] K. Shibata, “Measurement of Complex Permittivity for Liquid Materials Using the Open-ended Cut-off Waveguide Reflection Method,” IEICE Trans. Electron., Vol. E93-C, No. 11, pp. 1,621 – 1,629, 2010-11.

[2] K. Shibata, “Broadband Measurement of Complex Permittivity for Liquids Using the Open-ended Cut-off Circular Waveguide Reflection Method,” Proc. of 35th PIERS, Guangzhou, China, pp. 2,079 – 2,084, 2014-8.

[3] K. Shibata and M. Kobayashi, “Broadband Measurement of Complex Permittivity for Liquids via the Open-ended Cut-off Waveguide Reflection Method Using a Large-bore Connector,” Proc. of the 45th European Microwave Conf., EuMC 2015, Paris, France, pp. 979 − 982, 2015-9.

[4] K. Shibata and M. Kobayashi, “Simplification of Liquid Dielectric Property Evaluation Based on Comparison with Reference Materials and Electromagnetic Analysis Using the Cut-off Waveguide Reflection Method,” IEICE Trans. Electron., Vol. E100-C, No. 10, pp. 908 – 917, 2017-10.

[5] K. Shibata, “Method for Dielectric Measurement in Liquids Using an Estimation Equation without Short Termination,” Proc. of the 22nd International Microwave and Radar Conference, MIKON 2018, Poznan, Poland, pp. 751 – 754, 2018-5.

[6] K. Shibata, “Dielectric Measurement in Liquids Using an Estimation Equation without Short Termination via the Cut-Off Circular Waveguide Reflection Method,” IEICE Trans. Electron., Vol. E101-C, No. 8, pp. 627 – 636, 2018-8.

[7] K. Shibata, “Improvement in Liquid Permittivity Measurement Using the Cut-off Waveguide Reflection Method,” Proc. of the 1st European Microwave Conference in Central Europe, EuMCE 2019, Prague, Czech Republic, 2019-5.

[8] K. Shibata, “S11 Calibration Method for a Coaxial Line with Three Reference Materials and no Short Termination Condition for Dielectric Measurement in Liquids,” Proc. of URSI AP-RASC 2019, New Delhi, India, 2019-3.

[9] K. Shibata, “Effectiveness Confirmation for S11 Calibration Theory of a Coaxial Line Using Three Reference Materials Based on Actual Measurement and Application to Dielectric Measurement in Liquids,” IEICE Technical Report, Vol. 118, No. 218, MW2018-68, pp. 49 – 54, 2018-8.

[10] K. Shibata, “S11 Calibration Method for a Coaxial-loaded Cut-off Circular Waveguide Using SOM Termination,” Proc. of the 2020 IEEE Sensors Applications Symposium, IEEE SAS 2020, Kuala Lumpur, Malaysia, 2020-3.

[11] K. Shibata, “Dielectric Measurement in Liquids via the Cut-off Circular Waveguide Reflection Method after S11 Calibration Using SOM Termination,” Proc. of the 23rd International Microwave and Radar Conference, MIKON 2020, Vilnius, Lithuania, 2020-5 (accepted) (event rescheduled to 5 – 8 October 2020 at venue in Warsaw, Poland, due to COVID-19).

[12] S. Rehnmark, “On the Calibration Process of Automatic Network Analyzer Systems,” IEEE Trans. on Microwave Theory and Tech., Vol. MTT-22, No. 4, pp. 457 – 458, 1974-4.

[13] D. Rytting, “Network Analyzer Error Models and Calibration Methods,” Agilent Technology Application Note.

[14] “HP 8753D Network Analyzer User’s Guide,” Hewlett-Packard, HP part number 08753-90257, 1997-10.

[15] A. Kraszewski, M. A. Stuchly and S. S. Stuchly, “ANA Calibration Method for Measurement of Dielectric Properties,” IEEE Trans. Instru. and Meas., Vol. IM-32, No. 2, pp. 385 – 387, 1983-6.

[16] “HP 85070B Dielectric Probe Kit, User’s Manual,” Hewlett- Packard, HP part number 85070-90009, 1993-4.

[17] U. Kaatze, “Complex Permittivity of Water as a Function of Frequency and Temperature,” J. Chem. Eng. Data, 1989, 34 (4), pp. 371 – 374, 1989-10.

[18] T. J. Ikyumbur et al., “Optimization in the Computation of Dielectric Constant of Methanol Using Debye Relaxation Method,” British Journal of Applied Science & Technol. 19 (1), pp. 1 – 10, 2017-2.

[19] A. P. Gregory and R. N. Clarke, “Tables of the Complex Permittivity of Dielectric Reference Liquids at Frequencies up to 5 GHz,” NPL Report Mat. 23, 2012-1.

[20] K. Shibata and M. Kobayashi, “Difference Between the Method of Moments and the Finite Element Method for Estimation of Complex Permittivity in Liquids Using a Coaxial Probe,” Proc. of EMC Europe 2019, Barcelona, Spain, 2019-9.

[21] K. Shibata and M. Kobayashi, “Dielectric Property Measurement Errors Based on Application of an Estimation Equation Using the Coaxial Probe Method,” Proc. of the 7th IEEE MTT-S International Microwave & RF Conference, IMaRC 2020, Mumbai, India, 2019-12.

[22] K. Shibata “Uncertainty Analysis for S11 Calibration of a Coaxial Line with Three Reference Materials without Short Termination,” Proc. of the XXXIII General Assembly and Scientific Symposium of the International Union of Radio Science URSI GASS 2021, Rome, Italy, August, 2021.

要　旨

本報告書では，液体の誘電率測定の前段階での同軸給電の遮断円筒導波管の試料前面での S_{11} の校正に，Vector Network Analyzer （VNA）で一般的に用いる SOL（short, open, 及び loaded）の終端条件を適用した．その為，先ず S_{11} を 1 ポートにて校正する公式を定義した．次に、SOL での校正理論を示した．更に，同軸給電型遮断円筒導波管の内部における load（整合終端）の実現法を提案した。そして、提案した整合終端を用いた複数回の繰り返し測定時の反射特性および再現性を 0.50 – 3.0GHz の周波数帯域にて確認した。更に、0.50, 1.5 及び 3.0 GHz の各周波数で，同軸給電型遮断円筒導波管の S_{11} を SOL で校正後の各種終端条件（short, open, loaded および各種液体を挿入時）の S_{11} の測定値を、他手法にて S_{11} を校正後の測定値と比較して提案手法の妥当性を検証した。これを踏まえ、先の SOL にて校正後の試料前面での S_{11} の測定値から，電磁界解析（モード整合法）による S_{11} の計算値と比較する逆問題で各種液体の複素誘電率を推定した．そして，SOL にて校正後の複素誘電率の推定値を SOM にて校正後の複素誘電率の推定値と比較し、提案手法の有効性を確認した．更に，0.50 – 3.0GHz の周波数帯域で S_{11} を SOL 校正後のモード整合法の逆問題による各種液体の複素誘電率の周波数特性の推定値も，SOM で校正後の複素誘電率の周波数特性の推定値と比較した．その結果，両者は良好に一致した．これより，本論文で提案した S_{11} の校正法と誘電率測定法の妥当性が確認された．

キーワード ： 誘電率測定，液体，インピーダンス測定，同軸線路，遮断円筒導波管反射法，マイクロ波，高周波, S11，校正